Journal of the Serbian Chemical Society
JSCS-info@shd.org.rs • www.shd.org.rs/JSCS

J. Serb. Chem. Soc. 90 (10) 1189–1201 (2025)
JSCS–5448

Original scientific paper
Published 26 October, 2025

Investigation of multi-walled carbon nanotubes catalytic activity by means of the model aerobic oxidation reaction

NARMIN MUSTAFAYEVA*, ELDAR ZEYNALOV, ASGAR HUSEYNOV, YAGUB NAGİYEV, MEHPARA NADİRİ and MATANAT MAHARRAMOVA

Ministry of Science and Education of the Republic of Azerbaijan, Institute of Catalysis and Inorganic Chemistry named after Academician Murtuza Nagiyev, AZ1143 Baku, Azerbaijan

(Received 23 January, revised 30 March, accepted 3 August 2025)

Abstract: This study investigates the synthesis of multi-walled carbon nanotubes (MWCNTs) *via* chemical vapor deposition (CVD) using propane gas and evaluates their catalytic efficiency in oxidation reactions. The MWCNTs were synthesized in a laboratory-scale CVD reactor under optimized conditions, with ferrocene used as a precursor to incorporate 9.8 wt. % iron into the nanotube structure. The catalytic activity of the synthesized MWCNTs was evaluated in the cumene oxidation reaction, demonstrating remarkable performance even at relatively low temperatures. This enhanced catalytic efficiency is attributed to the presence of iron compounds within the MWCNT channels, which are presumed to act as active sites for the reaction. Among the catalysts studied, the G-CVD-1 sample containing 9.8 wt. % iron showed the highest performance, accelerating the oxidation reaction by a factor of 23 compared to the uncatalyzed process. In comparison, the L-CVD-184 sample, with a lower iron content of 3.7 wt. %, achieved a 16-fold increase in reaction rate relative to the same uncatalyzed baseline. These values indicate that the iron concentration within MWCNTs plays a crucial role in determining their catalytic efficiency, with higher iron loading providing significantly better activity. This study demonstrates that iron-modified MWCNTs possess significant potential as durable and efficient catalysts for oxidation reactions.

Keywords: metal-containing carbon nanotubes; CVD reactor; catalyst; cumene; kinetic parameters; oxygen rate.

INTRODUCTION

Carbon nanotubes (CNTs) have emerged as distinctive allotropes of carbon, exhibiting substantial applications across various domains, including technology and catalysis. Their applications predominantly encompass nanotechnology, nanomedicine,[1] transistors, actuators, sensors,[2] membranes and capacitors.[3]

* Corresponding author. E-mail: nabdurrehmanova@mail.ru
https://doi.org/10.2298/JSC250123061M

In recent years, carbon nanotubes have garnered significant attention in the realm of nanocatalysis, drawing extensive investigation from researchers worldwide. Notable characteristics of CNTs include their lightweight nature, diminutive size, coupled with high surface area, impressive tensile strength, non--toxicity, and excellent electrical conductivity. These properties render CNTs highly advantageous as fillers in diverse materials such as polymers, metal surfaces and ceramics.[4,5] Furthermore, numerous studies have demonstrated that the incorporation of various functional groups[6–11] and metal atoms[12–16] into CNTs yields catalysts with markedly enhanced catalytic activity compared to other carbon allotropes.

For instance, nitrogen-doped carbon nanotubes have been effectively utilized as catalysts in the aerobic oxidation of cyclohexane to adipic acid, along with its precursors, cyclohexanol and cyclohexanone.[17] Multi-walled carbon nanotubes have been directly employed by Wang and colleagues as more durable and environmentally friendly catalyst for the conversion of ethanol to acetaldehyde in the presence of molecular oxygen. The C=O groups generated on the nanocarbon surface have been identified as active sites for the selective oxidation of ethanol to acetaldehyde, achieving approximately 60 % ethanol conversion with 93 % selectivity for acetaldehyde at an optimized temperature of 270 °C. Notably, the catalytic activity exhibited remarkable stability over a duration of 500 h, comparable to that of supported gold catalysts. This robust catalytic performance underscores the potential industrial applications of CNTs in catalysis. Further investigations have revealed that nanocarbon materials function as effective catalysts for activating C–H bonds in carbon nanotubes, short-chain alkanes in either the gas or liquid phase or ethylbenzene. A prominent example is the oxidative dehydrogenation of ethylbenzene to styrene facilitated by oxygen atoms. The absence of strong Lewis acid metal cations minimizes coke formation, thus preserving catalyst activity.[18]

In another study, carbon nanotubes functionalized with oxygen-containing groups were developed as novel catalyst types (*e.g.*, V_2O_5/TiO_2–CNTs–OH, V/Ti–CNTs–OH, V_2O_5/TiO_2–CNTs–COOH, V/Ti–CNTs–COOH and V_2O_5/TiO_2––CNTs, V/Ti–CNTs). These catalysts were employed to catalytically degrade 1,2-dichlorobenzene at low temperatures (150 °C). The findings revealed that the modification with oxygen-containing functional groups significantly enhanced the catalytic activity of V/Ti–CNTs, particularly highlighting the exceptional performance of the V/Ti–CNTs–COOH catalyst at low temperatures.[19]

In a separate investigation, researchers focused on iron and nitrogen atoms, developing two distinct CNT catalysts: single-walled CNTs (Fe–N–SWCNT) and double-walled CNTs (Fe–N–DWCNT). They conducted both experimental and theoretical studies on CO_2 conversion, emphasizing the effects of electrical energy on CO_2 conversion with increasing CNT diameter. The study established

that Fe–N–DWCNT exhibited superior catalytic activity for CO_2 adsorption compared to Fe–N–SWCNT while maintaining catalyst stability. Notably, Fe–N––DWCNT demonstrated potential for selective HCOOH production from CO_2 conversion.[20]

Moreover, the catalytic activity of the Fe_2O_3/CNT catalyst in the selective oxidation of ammonia was examined in a constant flow reactor. Results indicated that the incorporation of iron(III) oxide onto carbon nanotubes effectively enhanced the electronic properties of the CNTs. Under the influence of this catalyst, NO conversion exceeded 90 % within a temperature range of 200–325 °C. Furthermore, studies indicated that the Fe_2O_3/CNTs catalyst displayed resistance to SO_2/H_2O, demonstrating considerable reaction stability.[21]

As highlighted, research into nanocarbon-based catalysts suggests their significant potential for industrial applications, presenting a viable alternative to metal-based catalysts with relatively high economic value. The field of nanocatalysis stands on the cusp of significant growth as a new area of inquiry. However, several limitations, particularly concerning production costs, impede the large--scale application of carbon nanotubes.[3]

Various methods have been employed for synthesizing carbon nanotubes, with parameters such as sample purity, structural integrity, surface area, surface load, particle size distribution, surface chemistry and agglomeration conditions significantly influencing the reactivity of CNTs.[22] The most widely accepted synthesis methods for carbon nanotubes include: 1) chemical vapor deposition,[23,24] 2) laser ablation[25,26] and 3) carbon arc discharge.[27–29] Each method presents distinct advantages and drawbacks; however, CVD is regarded as the most economically feasible approach for large-scale, high-purity CNT production, primarily due to its ability to yield high-purity samples and facilitate straightforward control of the reaction medium.[22,30]

The predominant hydrocarbon sources utilized in CNT production *via* the CVD method include petrochemical products such as methane, ethane and acetylene, as well as petroleum derivatives like natural gas and kerosene.[31] The selection of hydrocarbon precursors plays a critical role in determining the growth, physicochemical and thermodynamic properties of CNTs. The gas-phase synthesis method is particularly advantageous, yielding less contaminated CNTs while also permitting large-scale production.[32,33]

Given these considerations, the catalytic oxidation of hydrocarbons utilizing CNTs represents a novel priority, with ongoing developments in its fundamental and applied aspects. Nonetheless, the inefficiencies associated with large-scale CNT production remain a principal challenge. This article elucidates the production of carbon nanotubes from inexpensive raw materials and explores their catalytic activity in the oxidation reaction of isopropylbenzene.

EXPERİMENTAL

This study commenced with the synthesis of multi-walled carbon nanotubes from a gas feedstock (propane) through chemical vapor deposition in the gas phase. The selection of the propane gas mixture as a precursor for carbon nanotube synthesis is justified by its potential for multi-tonnage production within our country, as well as its ability to yield cleaner, flatter, and relatively larger carbon nanotubes.

To facilitate this process, an expanded laboratory setup was established, leading to the synthesis of various samples of MWCNT (G-CVD-1). The apparatus (Fig. 1) comprises five primary components.

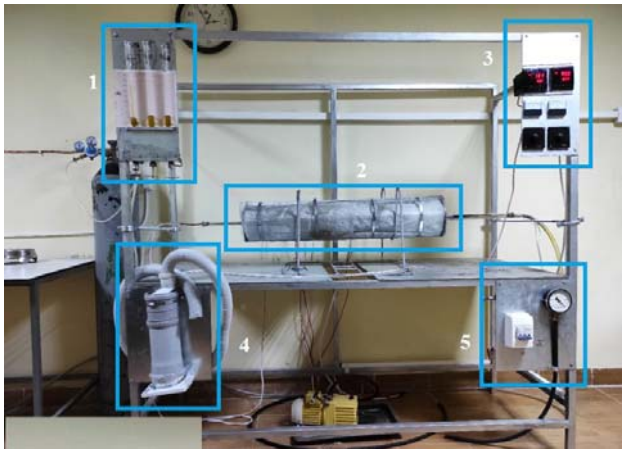

Fig. 1. MWCNT synthesis device; 1 – gas raw material preparation unit: the gas raw material (propane, butane, their mixture) is diluted with argon to the required concentration and fed to the reactor zone at a certain speed. 2 – Reactor block: it consists of 2 parts, each of which is heated independently by a tubular furnace with a quartz reactor inside. The furnace heats the reactor to a temperature of 1000 °C. 3 – Furnace temperature control unit block: this consists of a temperature regulator that automatically controls and maintains the set temperature in the reactor and two regulators to supply current to the furnace coil. 4 – air supply block. 5 – Vacuum block: to create a vacuum in the reactor, the block is designed for the synthesis of CNT at reduced pressures (80–20 kPa). The unit consists of a vacuum pump, a valve and a manometer.

Preparation of G-CVD-1 catalyst using chemical vapor deposition in the gas phase

During the process, propane gas is mixed with argon in the primary gas mixture preparation block. The flow rate of propane is $q_{propane}$ = 6 L h^{-1}, while that of argon is q_{argon} = 60 L h^{-1}, resulting in an argon-to-propane volume ratio of 10:1. The prepared gas mixture is directed into a quartz reactor housed within a furnace. In the first section of the reactor, the temperature is maintained at 200 °C. Here, 1 g of ferrocene is placed in a specialized ceramic container, where it serves as the precursor for the catalyst. At this stage, the argon-propane mixture is combined with ferrocene vapor and introduced into the second section of the reactor, where the temperature is increased to 900 °C. At 900 °C, ferrocene vapor undergoes decomposition, leading to the release of iron atoms, which form nanoscale clusters within the reactor. These clusters play a crucial role in the synthesis of carbon nanotubes. It is noteworthy that

the synthesis of carbon nanotubes primarily occurs via the growth mechanism facilitated by iron atoms derived from ferrocene. However, ferrocene itself does not directly participate in the reaction mechanism. These clusters act as catalysts during the synthesis process. Simultaneously, propane undergoes cracking in the second section of the reactor. The resulting carbon deposits grow on the Fe clusters, leading to the formation of multi-walled carbon nanotubes. Upon completion of the synthesis process, which lasts for 40–60 min, the flow of propane is stopped. The system is allowed to cool, after which the quartz tube is removed from the reactor (furnace). The MWCNTs deposited on the inner walls of the tube are collected using a metal rod. A fraction of the Fe catalyst used during the synthesis remains embedded within the MWCNTs. The mass fraction of the catalyst in the nanotubes was determined through combustion analysis.[34] The catalytic activity of the newly synthesized sample containing 9.8 wt. % Fe atoms (MWCNT (G-CVD-1)) was evaluated using the model reaction of cumene oxidation. Oxidation experiments were conducted in a gasometric device,[12,13] where molecular oxygen (atmospheric oxygen) was employed to investigate the kinetic characteristics of cumene oxidation. The measurements were carried out by the volumetric method, based on the rise of the liquid level in the burette due to the adsorption of oxygen. The total volume of the reaction mixture was 10 mL, and the reaction was conducted at a constant temperature of 60 °C. The oxygen pressure in the system was maintained at 20 kPa (under air atmosphere). As the reaction was performed in a gasometric setup without the use of any solvents (under pure conditions), the starting concentration of cumene reflects that of its undiluted liquid form at the specified conditions (≈ 6.9 mol L^{-1}).

These pressure values were selected to ensure that oxygen actively participates as a reactive component. Initially, the reaction was carried out under control conditions without the addition of carbon nanotubes to the reaction mixture. In this case, the catalyst sample was not involved in the reaction, and the reaction rate depended solely on the intrinsic properties of the reactants.

In the second stage, the reaction was performed by introducing the MWCNT (G-CVD-1) catalyst sample into the mixture at a concentration of 0.005 g L^{-1}. In the third stage, the MWCNT (G-CVD-1) catalyst was added at two different concentrations (0.01 and 0.02 g L^{-1}) to the reaction mixture. The volume of oxygen adsorbed during the reaction was the primary parameter used to evaluate the reaction rate and the efficiency of the catalyst. Using the same methodology,[13] investigations were conducted with the L-CVD-184 catalyst sample synthesized *via* the CVD method from a liquid carbon source, containing 3.7 wt. % Fe. Unlike the previous catalyst sample, the initiation of the reaction with L-CVD-184 involved the use of azobisisobutyronitrile (AIBN) as a radical initiator. AIBN decomposes at elevated temperatures, triggering the initiation stage of the reaction mechanism.

RESULTS AND DİSCUSSİON

The scanning electron microscope (SEM, Fig. 2A), transmission electron microscope (TEM, Fig. 2B) and energy-dispersive X-ray (EDX) imaging (Fig. 2C) of the synthesized MWCNT (G-CVD-1) are presented below.

The SEM image of the MWCNT (G-CVD-1) catalyst sample illustrates the surface and morphology of the synthesized multi-walled carbon nanotubes. The fibers or tubular structures visible in the image correspond to multi-walled carbon nanotubes, which are tubular carbon materials with diameters measured in nanometers and lengths in the micrometer range. The magnification factor used in

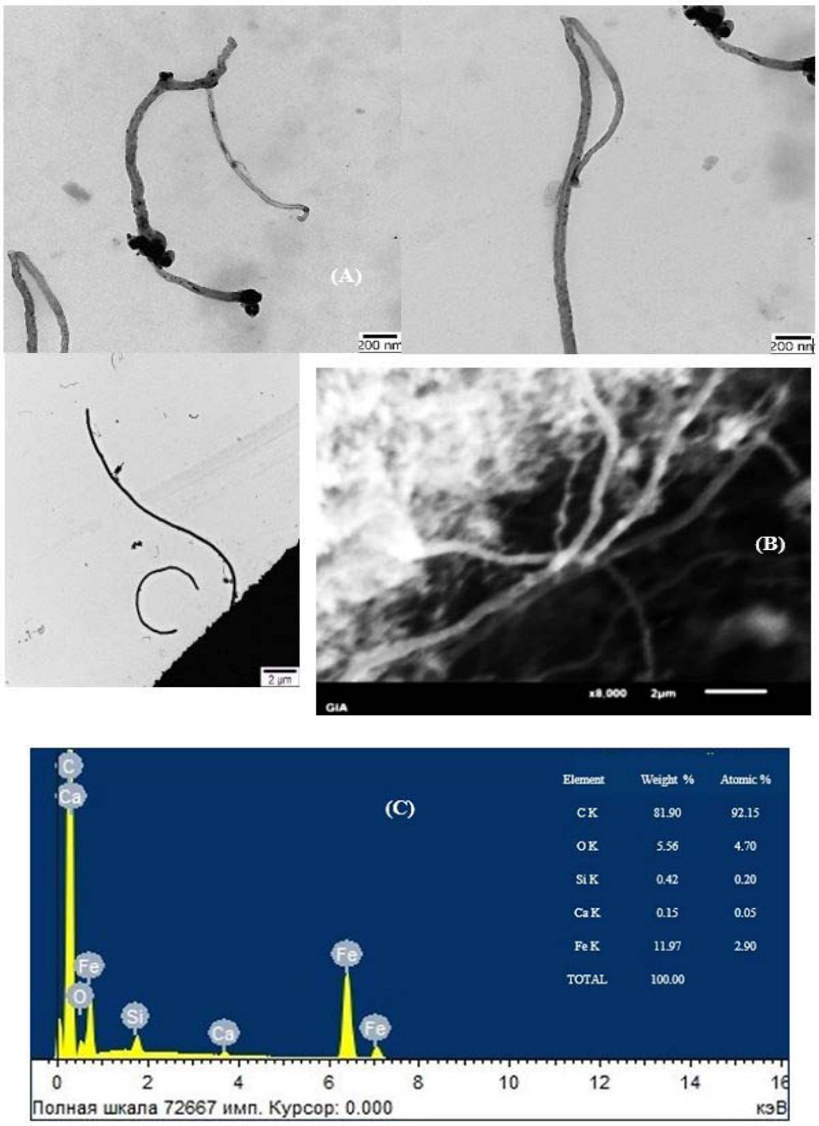

Fig. 2. Synthesized MWCNT (G-CVD-1) images: SEM (A), TEM (B) and EDX (C). (Scanning electron microscope JEOL, JSM6610LV. Oxford Instrument; Transmission Electron Microscope JEM-1400 (JEOL, Japan)).

the analysis was 8,000×, allowing for detailed observation of the sample's nanostructures. The diameters of the tubular structures range approximately from a few to 100 nm. The surface of the tubes appears smooth, indicating the high quality of the synthesis method. Furthermore, the tubes are observed to be entangled with one another, demonstrating their high surface area and nanoscale pro-

perties. As shown in the provided images, the synthesized MWCNT (G-CVD-1) exhibits a smooth surface, is free from visible defects, and features a linear morphology characterized by minimal bending and cracking. These observations suggest that the synthesized MWCNT (G-CVD-1) is of high quality and possesses minimal structural imperfections (Fig. 2A).

The TEM images depict the structural characteristics of the synthesized multi-walled carbon nanotubes (MWCNT (G-CVD-1)). The tubular structures, a defining feature of MWCNTs, are clearly visible. These structures consist of concentric graphene layers wrapped around each other. The images reveal that the MWCNTs are long, thin, and tubular in shape, with diameters measured on the nanometer scale (indicated by a 200 nm scale bar). In the first image, some of the tubes appear slightly bent or deformed. This deformation could be attributed to the conditions of the synthesis process or subsequent sample processing. In the second image, a straighter and more uniform tube is observed, indicative of a higher-quality structure with fewer defects. In both images, dark dot-like structures can be seen at the ends or along certain sections of the tubes. These are metal catalyst particles (Fe) used during the synthesis process. These particles act as nucleation points for the growth of MWCNTs, enabling carbon deposition through catalytic decomposition (Fig. 2B). The EDX analysis indicates that the primary component of the sample is carbon, comprising 81.90 mass % and 92.15 at. %. This confirms that the material is carbon-based. The iron content is measured at 11.97 mass % and 2.90 at. %, demonstrating the presence of iron in the sample, likely in the form of oxides (Fig. 2C).

Recent studies highlight that the unique physical properties of carbon nanotubes provide a solid foundation for the development of novel and efficient heterogeneous catalytic systems. Laboratory experiments have led to the creation of a new multi-walled carbon nanotube formulation containing iron, which exhibits high selectivity and efficiency. This catalyst serves as a versatile system, demonstrating significant effectiveness in the oxidation of various homologous hydrocarbons. The structural integrity of the MWCNT (G-CVD-1) catalyst, synthesized *via* the chemical vapor deposition method using propane, was confirmed through SEM analysis (Fig. 2A). Energy-dispersive X-ray spectroscopy analysis further revealed a substantial iron content (11.97 wt. %), emphasizing its critical role in the material. The incorporation of iron atoms during synthesis through the use of ferrocene as a catalyst precursor is particularly noteworthy.

In this study, the catalytic activity of iron-containing multi-walled carbon nanotubes in the aerobic oxidation reaction of cumene was analyzed. Experiments were conducted at a temperature of 60 °C, and the oxygen adsorption kinetics of the MWCNT (G-CVD-1) catalyst, synthesized from propane gas, were comparatively investigated to evaluate their effect on the oxidation reaction of

cumene. The catalyst contains 9.8 wt. % Fe, which significantly influences the reaction rate and kinetics.

Reaction rate without catalyst

The reaction rate without the catalyst was measured as $y = 0.0072x$. This value indicates that the reaction proceeds very slowly without a catalyst and can only occur at high temperatures and over a long period. The reaction under uncatalyzed conditions exhibits very low kinetics, which demonstrates the necessity of a catalyst to accelerate the process. From the given data, it is clear that the iron-containing MWCNT (G-CVD-1) catalyst lowers the activation energy of the reaction, significantly increases the reaction rate, and this effect is further enhanced as the iron content increases (Fig. 3).

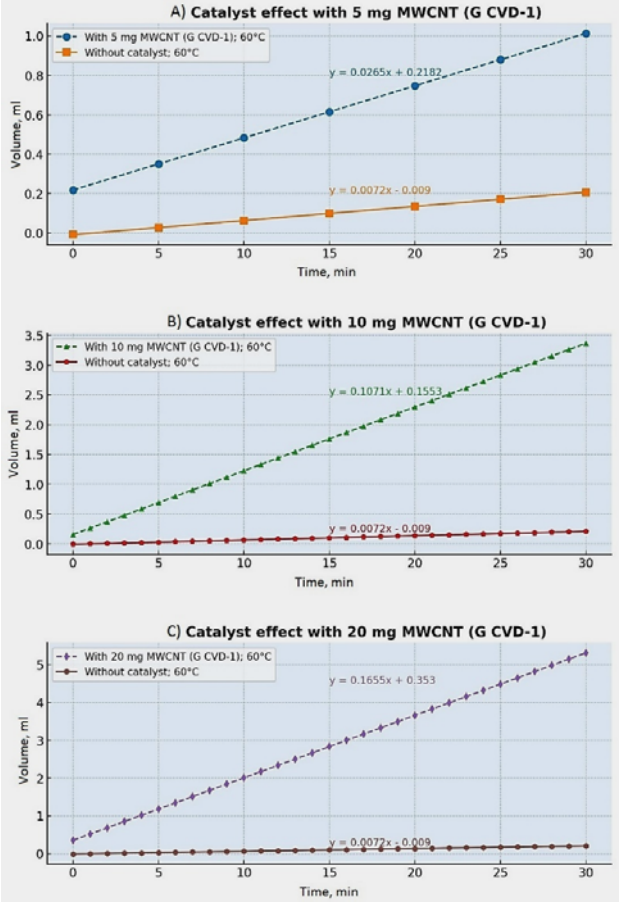

Fig. 3. Kinetic dependences of oxygen adsorption in aerobic oxidation reaction in the liquid phase of cumene in the presence of MWCNT (G-CVD-1) (9.8 wt. % Fe) catalysts synthesized from propane gas.

Effect of MWCNT catalyst quantity on reaction rate

In an experiment where 5, 10 and 20 mg quantities of MWCNT (G-CVD-1) catalyst were used, it was observed that as the quantity increased, the reaction rate also increased . With 5 mg of MWCNT (G-CVD-1) catalyst, the reaction rate was measured as $y = 0.0265x$ (Fig. 3A), while with 10 mg, it increased to $y = = 0.1071x$ (Fig. 3B). This caused the reaction to accelerate by approximately 3 and 15 times, respectively. With 20 mg of MWCNT (G-CVD-1), the oxygen adsorption rate further increased, and a 23-fold acceleration was observed, with $y = 0.1655x$ (Fig. 3C). This is due to the increase in the number of active sites on the catalyst surface as the amount of catalyst increases, leading to more collisions of reactive molecules with the surface, thus speeding up the reaction. However, when a certain threshold is reached, increasing the catalyst amount may not significantly affect the reaction rate. This is due to limitations related to the concentration of reactive species (substrate saturation).

Effect of Fe content on reaction rate

Experiments show that the high Fe content (9.8 wt. %) in the MWCNT (G--CVD-1) catalyst further accelerates the reaction compared to the MWCNT (L--CVD-184) catalyst sample with 3.7 wt. % Fe. The rate constant is 1.2 times higher (0.1304/0.1086 ≈ 1.2, Fig. 4). This difference can be explained by the following mechanism: Fe nanoclusters on the surface of the carbon nanotube exhibit high catalytic activity. It is clear that the catalyst sample with a higher amount of Fe nanoclusters (*e.g.*, 9.8 wt. % Fe) provides more active sites,

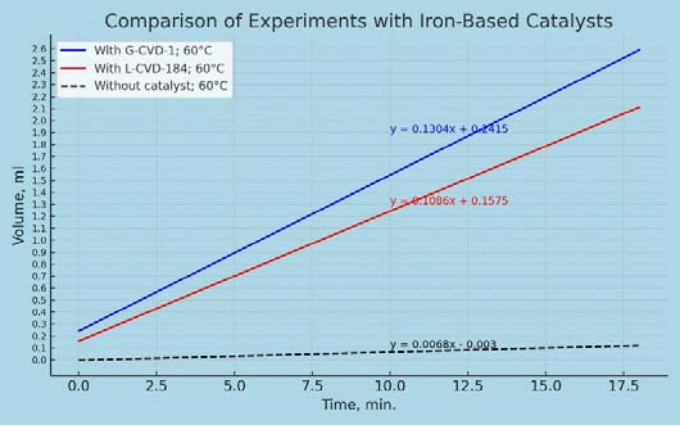

Fig. 4. Kinetic dependences of oxygen adsorption in the liquid phase aerobic oxidation reaction in the presence of catalysts MWCNT (G-CVD-1) and MWCNT (L-CVD-184) in the liquid phase of cumene. MWCNT (G-CVD-1) – carbon nanotubes synthesized from propane gas in the gas phase (9.8 wt. % Fe); MWCNT (L-CVD-184) – carbon nanotubes synthesized from cyclohexane in the liquid phase (3.7 wt. % Fe). Experimental conditions: cumene – 10 ml; AIBN – 10 mg; catalyst (G-CVD-1 or L-CVD-184) – 20 mg.

accelerating the reaction rate. More Fe clusters increase effective collisions with reactive molecules, thus reducing the activation energy and speeding up the reaction. This leads to the conclusion that Fe facilitates electron transfer in oxidation processes and promotes the formation of reactive oxygen species.

Reaction mechanisms and effective oxidation rate

The general pathway for the aerobic catalytic oxidation of cumene in the presence of MWCNT (G-CVD-1) is illustrated as follows, where Wo_2 represents the effective oxidation rate. The overall reaction steps (Eqs. (1)–(11)) follow the conventional numbering and notation system commonly used for hydrocarbon oxidation chain reactions in the scientific literature:[35,36]

Chain nucleation (formation of alkyl R$^\bullet$ radicals, rate W_o):

$$[R–H + M@MWCNT] \rightarrow R^\bullet + M@MWCNT\ (H) \quad (1)$$

$$[H\text{-}R\text{-}R\text{-}H + M@MWCNT] \rightarrow 2R^\bullet + M@MWCNT\ (2H) \quad (2)$$

$$RH + O_2 \rightarrow R^\bullet + HO_2^\bullet \quad (3)$$

$$2RH + O_2 \rightarrow 2R^\bullet + H_2O_2 \quad (4)$$

where M is a metal (Fe).

Continuation and development of the chain (rate W_d):

$$R^\bullet + O_2 \rightarrow RO_2^\bullet \quad (5)$$

$$RO_2^\bullet + RH \rightarrow ROOH + R^\bullet \text{ (rate constant } k_3) \quad (6)$$

The presence of a carbon nanocatalyst results in the decomposition of the intermediate catalytic complex (hydroperoxide–Fe@MWCNT), leading to the formation of additional active radicals and the propagation of the reaction chain according to the following mechanism:

$$ROOH + Fe@MWCNT \rightarrow [ROOH{*}Fe@MWCNT{*}ROOH] \rightarrow \rightarrow RO^\bullet + 2HO^\bullet + Fe^{2+} \quad (7)$$

$$Fe^{2+} + ROOH \rightarrow RO^\bullet + HO^- + Fe^{3+} \quad (8)$$

$$ROOH + Fe^{3+} \rightarrow 2Fe^{2+} + RO_2^\bullet + H^+ \quad (9)$$

Open circuit (rate W_t):

$$RO^\bullet + RO^\bullet/RO_2^\bullet + RO_2^\bullet \rightarrow \text{Radical recomb. prod. (rate constant } k_6) \quad (10)$$

The kinetic equation that describes the proposed scheme can be represented as follows:

$$Wo_2 = (W_o + W_d)^{1/2} k_3 k_6^{1/2} [RH] \quad (11)$$

The high surface area of such nanotube structures provides more active sites, ensuring more reactions occur. The catalytic role of Fe makes the reaction faster and more efficient, which increases the potential for using MWCNTs in industrial oxidation processes.

CONCLUSION

In conclusion, this study investigated the catalytic properties of iron-containing multi-walled carbon nanotubes (MWCNT (G-CVD-1)) and determined that they significantly accelerate the aerobic oxidation reaction of cumene. The presence of 9.8 wt. % Fe in the MWCNT (G-CVD-1) catalyst increases the number of active sites, thereby exerting a strong effect on the reaction kinetics. The increase in catalyst quantity and Fe content enhanced the reaction rate by approximately 23 times and 1.2 times, respectively. The results of this study suggest the promising application of MWCNT catalysts as highly efficient materials for industrial oxidation processes.

ИЗВОД

ı óÖ°—° ı ª—" Œ#—Ö—ø ı Öı ¬ł Œ#–ł Öı ª ß ¹ óÖı #' ı Ë Œóø ¹ ‰ß ı û#Ð Ł¤ Œß ı ¬ß ı û# ß—ß ¹ ¼ Œª ı #– ¹ œ ¹ « ö#e ¹ ØŒø#–Œ° ¹ ÆßŒ#'Œ—ł¼ ı ‰Œ# ł ó ı Ø—¼ ı ‰Œ#

NARM IN #M USTAFAYEVA ,#ELDAR #ZEYNALOV ,#ASGAR #HUSEYNOV ,#YAGUB #NAGİYEV ,#M EH PARA #NADİRİ# |#MATANAT #M AHARRAM OVA#

M hmhnsqx#ne#Sbhdmbd#'mc#Ectb'shnm#ne#kgd#Rdbtalkbd#ne#Aydqa'hi'm,#fmmshnt sd#ne#B 's'kcdh#'mc#fmnqf'mlbd# Bgdl hnsqx#m'l dc#'esdg#Ab'cdl hbh'm#M tqsty'#N 'fhxdu,#AZ0032#B 'jt,#Aydqa'hi'm#

¹ úÇ# |Åµð½î |ú½" Ð# Ð# ÙÅý ÐõÐÁÇ# Á½# Å|ÁµÐ®Ù# ú|Ú ÐÅÃÇ ̃Á|Š# Ùé, ÐÁ|ÑÁ|Š# Á½ÁÇõÐú|# (M W BN T)#ñÙµÐý #ŠÐý |ˆÅþÐ#ŁÐñÇ®|õ| Ð#|®#ñ½ÐÐ#(BVD)#þÇð|Ú »Ð" Ðý #ê½Å½#ñðÇñ½Á½#| #ÇíõÐ-›|ú½" Ð#" |ŠÇúÐ#þ½µ½Ã|µ|ÑþÐ#ÐÈ |þ½ÅÁÇÅµ|#Ù#ðÐ½þõ| ¼ý ½#ÇþÅ|í½õ| Ð.#M W BN T#ÅÙ#Å|ÁµÐ-µ|Å½ÁÐ#Ù#Ã½ÕÇõ½µÇð| ˆÅþÇý #BVD #ðÐ½þµÇðÙ#ñÇí#Çñµ|ý |®Çú½Á|ý #ÙÃÃÇú|ý ½,#Ù®#þÇõ|Ú »Ð" Ð# È ÐðÇõÐÁ½#þ½Ç#ñõÐþÙðÅÇõ½®½#Ùéõ½í" Ù#9 ,8#ý½Å.#‰ #éúÇî ›½#Ù#ÅuðÙþµÙðÙ#Á½ÁÇõÐú| .#– Çþ½®½Á½# Ð#| ®Ù®ÐµÁ½#þ½µ½Ã|µ|ÑþÐ#¼þµ|úÁÇÅµ#Å|ÁµÐµ|Å½Á|Š#M W BN T#®½#Ç þÅ|í½õ| Ù#þÙý ÐÁ½,#Ñ¼þ#| #Á½# ðÐÃ½µ|úÁÇ#Á|Åþ|ý #µÐý ñÐð½µÙð½ý ½.#¹ ú½#ñÇÕÇ, Ú ½Á½#þ½µ½Ã|µ|ÑþÐ#ÐÈ |þ½ÅÁÇÅµ#ñð|ñ|ÅÙ Ð# Åð#ñð|ÅÙÅµúÙ#Ðí|" Ð" ½#éúÇî ›½#ÙÁÙµ½ð#M W BN T#þ½Á½Ã½,#®½#þÇ ̃½#Åð#ñðÐµñÇÅµ¼í, ½#ł½#ŁÐÃÙ Ù# þ½Ç#¼þµ|úÁ½#ý ÐÅµ¼#®½#ðÐ¼þõ| Ù.#e Ð›Ù#ñðÇÙÑ½ú½Á|ý #þ½µ½Ã|®½µÇõ|ý ½,#Ù®Çð½þ#G –BVD –0#þÇ ̃|# Å½íðî |#9 ,8#ý½Å.#‰ #éúÇî ›½#ñÇþ½®½Ç#Ð#Á½ÕÇ, Ð#ñŁðÈ ÇðÝ ½ÁÅÐ,#ÙÕð®½ú½Ù» |#ðÐ½þõ| Ù#ÇþÅ| -í½õ| Ð#22#ñÙµ½#Ù#ñÇðÐ›Ð" Ù#Å½#ÁÐþ½µ½Ã|®Çú½Á|ý #ñðÇõÐÅÇý .#– ÇðÐ›Ð" ½#ð½í| ,#Ù®Çð½þ#L-# -BVD –083 ,#Å½#Á|î |ý #Å½íðî ½Ðý #éúÇî ›½#Çí#2 ,7#ý½Å.#‰ ,#ñÇÅµ|ê½Ç#Ð#06#ñÙµ½#úÐ»Ù#ÕðÝ®|ÁÙ# ðÐ½þõ| Ð#Ù#Ç íÁÇÅÙ#Á½#| ÅµÙ#ÁÐþ½µ½Ã|®Çú½ÁÙ#ÐÐþ½õ| Ù.#ú|#ÐÐ®ÙÃµ½µ|#Ùþ½®Ù Ù#Á½#µÇ#Í½#þÇÁ-õÐÁµðí½õ| ¼#éúÇî ›½#ÙÁÙµ½ð#M W BN T#|éð½#ú½î ÁÙ#ÙÃÇéÙ#Ù#Çíðð›|ú½" Ù#" |ŠÇúÐ#þ½µ½Ã|µ|ÑþÐ# ÐÈ |þ½ÅÁÇÅµ| #ñð|#ÑÐý Ù#úÐ»Ð#þÇÁõÐÁµðí½õ| Ð#éúÇî ›½#ÇÕÐ®ÕÐ›Ù Ù#®Á½ÁÇ#ÕÇ, Ù#¼þµ|úÁÇÅµ.# ¹ ú½#Åµùí| ¼#ñÇþ½®Ù Ð#Í½#M W BN T#ýÇí|È |þÇú½ÁÐ#éúÇî ›Ðý #ñÇÅÐíÙ Ù#®Á½Ñ½½Á#ñÇµÐÁõ | ¼Ã# þ½Ç#| ®íðî , |ú|#|#ÐÈ |þ½ÅÁ|#þ½µ½Ã|®½µÇð|#®½#ÐÐ¼þõ| Ð#ÇþÅ|í½õ| Ð.#

(– ð|ý , ÐÁÇ#2 .#½ÁÙ½ð½,#ÐÐú|í|ð½Á Ç#20 .#ý ½ð,µ½,#ñð|Šú½»ÐÁÇ#2 .#½éÙÅµ½#2025)#

REFERENCES

1. M. Daniyal, B. Liu, W. Wang, *Curr. Med. Chem.* **27** (2020) 3665 (https://doi.org/10.2174/1381612825666190201129629O)
2. B. D. Gupta, A. Pathak, V. Semwal, *Sensors* **19** (2019) 3536 (https://doi.org/10.3390/s19163536)
3. M. Melchionna, S. Marchesan, M. Prato and P. Fornasieroa, *Catal. Sci. Technol.* **5** (2015) 3859 (https://doi.org/10.1039/C5CY00651A)

4. Y. Yibo, M. Jianwei, Y. Zhihong, X. Fang-Xing, H. B. Yang, B. Liu, Y. Yang, *Chem. Soc. Rev.* **44** (2015) 3295 (https://doi.org/10.1039/C4CS00492B)
5. I. Khan, Kh. Saeed, *Carbon Letters* **14** (2013) 131 (https://doi.org/10.5714/CL.2013.14.3.131)
6. A. Sivaranjani, C. Lakshmi Devi, *Mater. Res. Express* **6** (2019) 1050e3 **(**https://doi.org/10.1088/2053-1591/ab42ff)
7. E. B. Zeynalov, E. R. Huseynov, N. I. Salmanova, N. A. Abdurahmanova, *Chem. Probl.* **3** (2020) 351 (https://doi.org/10.32737/2221-8688-2020-3-351-360)
8. E. B. Zeynalov, Y. M. Nağıyev, F. M. Mammedov, S. A. Alıyeva, M. I. Nadırı, L. I. Ahmedova, M. Y. Maharramova, N. A. Abdurehmanova, G. Sh. Asadzade, *News Baku State Univer.* **1** (2017) 18 (http://static.bsu.az/w1/pdf%202017%20N1/1.pdf)
9. N. A. Mustafayeva, *Azer. Chem. J*. **2022** (2022) 87 (https://doi.org/10.32737/0005-2531-2022-3-87-92)
10. Ya. M. Nagiyev, *Proc. Petrochem. Oil Ref.* **1** (2021) 99 (https://www.ppor.az/jpdf/8-Naghiyev-1-2021.pdf)
11. E. B. Zeynalov, A. B. Huseynov, S. G. Abdullayeva, N. A. Abdurahmanova, in *Proceedngs of 6th International Caucasian Symposium on Polymers and Advanced Materials,* 2019, Batumi Shota Rustaveli State University, Georgia, Ivane Javakhishvili Tbilisi State University Press, Batumi, 2019, p. 115 (https://www.icsp6.tsu.ge/ge/x3_185s4csfh92rm)
12. N. A. Abdurahmanova, *Proc. Petrochem. Oil Ref.* **21** (2020) 268 (https://ppor.az/jpdf/11-Abdurahmanova-2-2020.pdf)
13. E. Zeynalov, A. Huseynov, E. Huseynov, N. Salmanova, Y. Nagiyev, N. Abdurakhmanova, *Chem. Chem. Technol.* **15** (2021) 479 (https://doi.org/10.23939/chcht15.04.479)
14. E. B. Zeynalov, Ya. M. Nagiyev, A.B. Huseynov, M. I. Nadiri, M. Kh. Abbasov, A. D. Guliyev, N. Salmanova, *SOCAR Proc.* **4** (2022) 134 (https://proceedings.socar.az/uploads/pdf/89/10.5510_OGP20220400794.pdf)
15. Ya. M. Nagiev, R. R. Apaeva, M. I. Nadiri, A. B. Guseinov, E. B. Zeynalov, *SOCAR Proc.* **3** (2023) 182 (https://doi.org/10.5510/OGP20230300900)
16. E. B. Zeynalov, N. S. Allen, Ya. M. Naghiev, A. B. Huseinov, F.G. Rzaev, *J. Phys. Chem. Solids* **195** (2024) 112263 (https://doi.org/10.1016/j.jpcs.2024.112263)
17. H. Yu, F. Peng, J. Tan, X. Hu, H. Wang, J. Yank, W. Zheng, *Angew. Chem. Int. Ed*. *Engl.* **50** (2011) 3978 (https://doi.org/10.1002/anie.201007932)
18. W. Jia, H. Rui, F. Zhenbao, L. Hongyang, S. Dangsheng, *ChemSusChem* **9** (2016) 1820 (https://doi.org/10.1002/cssc.201600234)
19. W. Qiulin, Z. Jianchao, T. Minghui, P. Yaqi, D. Cuicui, Y. Jianhua, L. Shengyong, *Environ. Prog. Sustain.* **38** (2019) 13221 (https://doi.org/10.1002/ep.13221)
20. H. S. Yoon, P. Hyunwoong, O. N. Elbashir, H. S. Dong, *Sust. Mat. Tech.* **26** (2020) e002244 (https://doi.org/10.1016/j.susmat.2020.e00224)
21. Q. Zhenping, M. Lei, W. Hui, F. Qiang, *Chem. Commun.* **51** (2015) 956 (https://doi.org/10.1039/C4CC06941B)
22. E. Ali, D. Hadis, K. Hamzeh, K. Mohammad, N. Zarghami, A. Akbarzadeh, M. Abasi, Y. Hanifehpour, S. W. Joo, *Nanoscale Res. Let.* **9** (2014) 393 (https://doi.org/10.1186/1556-276X-9-393)

23. E. Abbasi, F. A. Sedigheh, A. Abolfazl, M. Morteza, H. T. Nasrabadi, S. W. Joo, Y. Hanifehpour, K. Nejati-Koshki, R. Pashaei-Asl, *Nanoscale Res. Let.* **9** (2014) 247 (https://doi.org/10.1186/1556-276X-9-247)
24. Y. M. Jose., Y. M. Miki, L. Rendon, J. G. Santiesteban, *Appl. Phys. Lett*. **62** (1993) 202 (https://doi.org/10.1063/1.109315)
25. L. Chico, V. H. Crespi, L. X. Benedict, S. G. Louie, M. L. Cohen, *Phys. Rev. Lett.* **76** (1996) 971 (https://doi.org/10.1103/PhysRevLett.76.971)
26. P. M. Ajayan, T. W. Ebbesen, *Rep. Prog. Phys*. **60** (1997), 1025 (https://doi.org/10.1088/0034-4885/60/10/001)
27. A. Thess, R. Lee, P. Nikolaev, H. Dai, P. Petit, J. Robert, C. Xu, H. L. Young, G. K. Seong, A. G. Rinzler, D. T. Colbert, G. E. Scuseria, D. Tománek, J. E. Fischer, R. E. Smalley, *Science* **273** (1996) 483 (https://doi.org/10.1126/science.273.5274.483)
28. R. Hirlekar, M. Yamagar, H. Garse, M. Vij, V. Kadam, *Asian J. Pharm. Clin. Res.* **2** (2009) 17 (https://www.innovareacademics.in/journal/ajpcr/Vol2Issue4/238.pdf)
29. P. X. Hou, S. Bai, Q. H. Yang, C. Liu, H. M. Cheng, *Carbon* **40** (2002) 81 (https://doi.org/10.1016/S0008-6223(01)00075-6)
30. S. P. Patole, P. S. Alegaonkar, H. C. Lee, J. B. Yoo, *Carbon* **46** (2008) 1987 (https://doi.org/10.1016/j.carbon.2008.08.009)
31. A. Hayder, R. Irmawati, I. Ismayadi, Y. Nor Azah, *Pertanika J. Sci. Technol.* **25** (2017) 379 (https://www.researchgate.net/publication/316988879_Hydrocarbon_Sources_for_the_Carbon_Nanotubes_Production_by_Chemical_Vapour_Deposition_A_Review)
32. E. T. Thostenson, Z. Ren, T. W. Chou, *Comp. Sci. Technol*. **6** (2001) 1899 (https://doi.org/10.1016/S0266-3538(01)00094-X)
33. R. J. Hynes, R. Sankaranarayanan, M. Kathiresan, P. Senthamaraikannan, in *Nanocarbon and its Composites*, A. Khan, M. Jawaid, Inamuddin, A. M. Asiri, Eds., Woodhead Publishing, Cambridge**,** 2019, pp. 805–830 (https://doi.org/10.1016/B978-0-08-102509-3.00027-4)
34. Federal Agency for Technical Regulation and Metrology (OOO EO Engineering Safety), +7 and R 58356, 2019 (ГОСТ Р 58356-2019: Наноматериалы. Нанотрубки углеродные одностенные. Технические требования и методы испытаний (standartgost.ru))
35. N. S. Kobotaeva, T. S. Skorokhodova, N. V. Ryabova, *Russ. J. Phys. Chem., A* **89** (2015) 462 (https://doi.org/10.1134/S0036024415030164)
36. A. Bhattacharya, *J. Chem. Eng.* **137** (2008) 308 (https://doi.org/10.1016/j.cej.2007.04.043).